ORIENTAL JOURNAL OF CHEMISTRY
An International Open Access, Peer Reviewed Research Journal
www.orientjchem.org
ISSN: 0970-020 X
CODEN: OJCHEG
2025, Vol. 41, No.(2):
Pg. 471-481

Adsorptive Fluoride Removal using Zirconium-infused Agar-agar Based activated Biochar Derived from *Ricinus communis* Leaves (Zr-AAABC)

PRIYA TANWAR, DINESH DEORA, BHAWANA ARORA and PALLAVI MISHRA*

Department of Chemistry, Jai Narain Vyas University, Jodhpur 342001, India.
*Corresponding author E-mail: pallavianuk@gmail.com

http://dx.doi.org/10.13005/ojc/410216

(Received: December 16, 2024; Accepted: March 09, 2025)

ABSTRACT

Excess fluoride in drinking water poses significant health risks, necessitating the development of efficient and sustainable removal methods. This study investigates using a novel hybrid material, zirconium-loaded agar-agar-based activated biochar (Zr-AAABC), derived from Ricinus communis leaves, for fluoride removal from a water-based solution. The Zr-AAABC was synthesised by impregnating biochar from castor tree leaves with zirconium metal ions, utilising chemical and thermal activation techniques, including a 24-h treatment with 2M sulfuric acid. Temperature (20-90°C), adsorbent dose (0.1-1.5 mg/L), adsorption duration (10-180 min), pH levels (1-13), and initial concentration of fluoride (10-100 mg/L) were among the variables tested to determine Zr-AAABC's adsorption performance. We validated the bio adsorbent's composition and structure using SEM, FTIR and ImageJ software. The results of the adsorption experiment, which demonstrated a good match with the Langmuir isotherm model and pseudo-second-order kinetic model, are consistent with monolayer adsorption on a homogeneous surface. The optimal parameters for fluoride removal were as follows: 1 g adsorbent dose, 2 h of contact time, 60°C temperature, 10 mg/L starting fluoride concentration, and pH 7. We obtained 92% fluoride removal under the above conditions. However, we obtained only 82% fluoride removal using activated castor leaf biochar. Our results suggest that Zr-AAABC provides a sustainable and efficient alternative to conventional water filtration methods, including standard biochar, with significant potential for fluoride removal.

Keywords: Ricinus communis leaves, Agar-agar, Zirconium, Adsorption, Fluoride, Activated biochar.

INTRODUCTION

Tissue mineralization is essential for developing strong bones and tooth enamel and requires fluoride in all living organisms. Nevertheless, dental fluorosis and impaired calcium & phosphorus metabolism in both children & adults may result from excessive fluoride levels in drinking water[1]. This might impede the growth and development of youngsters. Concerned about these problems, the World Health Organization recommends keeping fluoride levels in water supplies between 0.5 mg/L and 1.5 mg/L[2]. Fluoride contamination is a significant issue as it affects over 200 million people globally,

particularly in developing countries with high fluoride water supplying fluoride, such as Iran, Kenya, China, and India. This issue is especially severe in some Indian states, including Uttar Pradesh, Gujarat, Andhra Pradesh, Karnataka, and Tamil Nadu[3]. For fluoride, developing a system to remove fluoride from potable water is essential for human and environmental health.

Ion exchange, coagulation, precipitation, electrodialysis, reverse osmosis, and adsorption are among the numerous methods that have been proposed for the removal of fluoride from potable water[4]. Adsorption is a method that is frequently employed and beneficial because of its simplicity and easy use, low energy consumption, cost-effectiveness, and high efficiency[5]. The creation of carbon-based adsorbents, such as activated C, C nanotubes, and carbon fibre made of affordable basic materials and enormous surface areas, for example, activated C, C nanotubes, and C fibre that are made of affordable basic materials and have vast surface areas has drawn the attention of several researchers. However, the limited physical interactions between fluoride and the adsorbents continue to hinder the adsorption capacity of these carbon adsorbents. This restriction has been overcome by adding metal hydroxides and oxides[6], which have significantly increased the surface area and interactions with fluoride, improving the carbon adsorption capacities. Another way to remove fluoride is using adsorbents filled with common metal ions[7], such as Zr^{4+} [8], Al^{3+} [9], Fe^{3+} [10], and La^{3+}.

This study introduces a cost-effective and innovative bioadsorbent, Zr-AAABC, developed by incorporating zirconium ions loaded agar-agar[11] based activated biochar derived from castor leaves. The impregnation process, performed via soaking, is a well-known method for modifying carbon-based adsorbents. Zirconium[12-15] is highly valued for fluoride adsorption due to its cost-effectiveness, non-toxicity, chemical stability, thermal resistance, and biocompatibility. As Zr (IV), its strong favourable electron properties enhance binding with fluoride ions through Lewis's acid-base interactions. When activated carbon is modified with zirconium ions, fluoride adsorption capacity increases 3-5 times, improving surface area, cavity volume, and active sites for efficient fluoride removal from water. Incorporating agar-agar in synthesising zirconium-loaded castor leaf biochar (Zr-AAABC) significantly enhances the adsorbent's properties and performance, especially for applications like fluoride removal from water. Agar-agar, a natural polysaccharide, contributes to the biochar's porosity during its preparation. This helps form a more porous structure with a higher surface area, essential for enhancing the material's adsorption capacity. The increased surface area provides more active sites for the adsorption of fluoride ions and other contaminants from water. Agar-agar acts as a binder in the composite material, improving the mechanical stability of the biochar[16,17]. This process can increase the bioadsorbent's surface area by up to tenfold, enhancing its fluoride removal capacity.

Zr-AAABC was systematically characterised using SEM-EDX, Image J, and FTIR analysis. Batch adsorption studies examined initial fluoride concentration, temperature, pH, adsorbent dosage, etc. Additionally, adsorption isotherms (Langmuir, Freundlich, and Temkin isotherms) and kinetics models (pseudo-first-order, pseudo-second-order, and Intra-particle diffusion models) were performed.

MATERIALS AND PROCEDURES

Development of materials

Reagents used

The reagents used during the experiments were Sodium Fluoride (97% assay, ASES Laboratory reagent), Zirconium Oxide (99% assay, HIMEDIA), Agar Agar powder no. 1 (LOBA Chemie), NaOH, and HCl, all of which were of analytical grade.

Fluoride stock and standard solution preparation

0.221 g of dry sodium fluoride was dissolved in 1000 mL double-distilled water in a volumetric flask, producing the 100-ppm fluoride stock solution. 100 mL of the stock solution was mixed with 1000 mL of double-distilled water to create the 10-ppm fluoride standard solution. The concentration of fluoride in this 1 mL solution was 0.1 mg.

Synthesis of Zr-AAABC

Matured leaves of *R. communis* were collected, cleaned adequately with distilled water, and then allowed to dry for three to four days. The dried leaves were powdered using an electrical grinder and pyrolysed entirely for 30 to 40 min at 400^0C in a muffle furnace. The biochar obtained

was activated with a 2M sulfuric acid solution. The activated biochar was first cleaned and washed extensively with deionised water until pH seven was obtained, after which it was dried in an oven for 12 h at 105^{0}C. A magnetic stirrer was used to mix 2 g activated charcoal with agar-agar (2%) solution. Later, 2% $ZrOCl_2 \bullet 8H_2O$ solution was gradually mixed into the agar-agar+activated biochar solution with constant stirring. The mixture was held at 85^{0}C for 3 h, and later, its temperature was raised to 110^{0}C for complete evaporation till our bioadsorbent was obtained. Activated charcoal functionalised with sulfuric acid introduces several surface functional groups, including sulfonic acid ($-SO_3H$), carboxyl (-COOH), and hydroxyl (-OH) groups, primarily through oxidation and sulfonation reactions. The $-SO_3H$ group, characteristic of sulfuric acid activation, significantly enhances the charcoal's adsorption capacity, especially for essential compounds. The functionalized charcoal is further modified by coating it with agar-agar, a polysaccharide forming a hydrogel-like network on the surface. Zirconium ions (Zr^{4+}) from zirconium oxychloride $ZrOCl_2 \bullet 8H_2O$ interact with the surface groups ($-SO_3H$, -COOH, and -OH), forming coordination complexes where these functional groups act as ligands, binding Zr^{4+} ions to the surface. The resulting zirconium-loaded biochar demonstrates enhanced fluoride (F^-) ion adsorption. The adsorption occurs through three mechanisms: electrostatic attraction, where the positively charged Zr^{4+} sites attract negatively charged F^- ions; ion exchange, where F^- displaces other anions (such as -OH) bound to zirconium; and surface complexation, where fluoride forms stable Zr-F bonds via inner-sphere complexation.

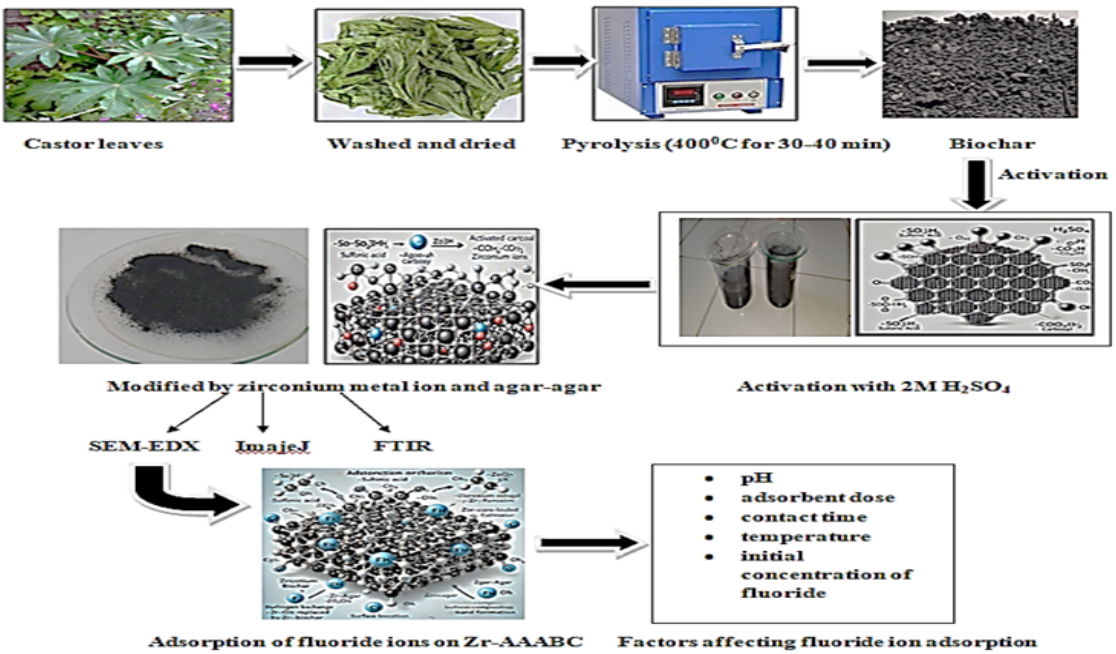

Fig. 1. Steps in synthesising zirconium-loaded, agar-agar-based castor leaves activated charcoal

Characterization methods

The surface morphology and structural features of Zr-AAABC were studied pre- and post-fluoride adsorption under scanning electron microscopy (SEM, Carl Zeiss Evo MA25). EDX (Energy-Dispersive X-ray Spectroscopy) was used to determine the element composition in Zr-AAABC. Fourier Transform Infrared Spectroscopy (FTIR, Agilent Cary 630) showed functional group adsorption in the 400-4000 cm^{-1} range. Using ImageJ software, the average pore size and length of the Zr-AAABC bioadsorbent were also measured before and after fluoride adsorption.

Adsorption study and fluoride measurement

For investigating fluoride adsorption onto Zr-AAABC, The optimal adsorption conditions were determined by adjusting the initial concentration of fluoride(10 to 100 mg/L), pH (1-13), temperature (20-90^{0}C), contact duration (10-180 min), adsorbent quantity range of (0.1-1.5 g/L) in the testing. The OFAT (one factor at a time) method, which

included changing one variable while keeping the others constant, was used to carry out the cohort studies. A 100 mL solution of 10 ppm fluoride solution was used in each adsorption experiment. A fluoride-selective electrode was used to measure the remaining concentration of fluoride. Ten to 180 min of kinetic adsorption was investigated with a starting concentration of fluoride, i.e. 10 mg/L, and an adsorption amount of 1 g/L, and Variations in fluoride content from 10-100 mg/L allowed one to investigate the adsorption isotherm at a 1 g/L adsorbent dosage. Here is the formula that was used to compute the capacity of adsorption (q_t, mg/g) of Zr-AAABC.

$$q_t = (C_0\text{-}C_t)V/m$$

C_0 = initial concentration of fluoride(mg/L)
C_t = currentconcentration of fluoride (mg/L)
V = solution's-volume (mL).
m = adsorbent quantity (g)

RESULTS AND INTERPRETATION

Characterisation of Zr-AAABC

Morphology and element detection

SEM analysis

Through the use of SEM analysis, the surface morphology of the Zr-AAABC was confirmed. The images obtained from the SEM of Zr-AAABC before & after fluoride adsorption are shown in Fig. 2(a) and (b). Significant pores are seen in the surface morphologies of Zr-AAABC, but the fluoride-loaded adsorbent reveals essentially minimal pores following fluoride adsorption. Consequently, the considerably developed pore structures and fluoride attachment capacity of Zr-AAABC are validated. The surface of Zr-AAABC smoothed out significantly more after fluoride ions saturated it, indicating that Zr-F complexes could potentially obstruct Zr-AAABC's Chanel.

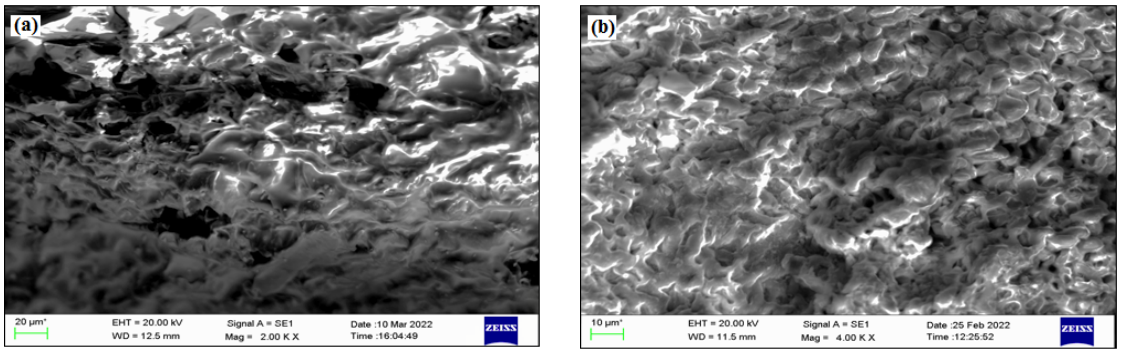

Fig. 2. Zr-AAABC SEM images- Before (a) and after adsorption (b)

Image J analysis

According to the figures, the adsorbent's surface was porous before adsorption, but after adsorption, the porosity significantly decreased, which can be attributed to fluoride adsorption. Image software demonstrated this phenomenon, showing that the adsorbent's surface area decreased as well (Fig.3), as demonstrated by the length and area of the pores, which were 19.10 micrometres and 6.479 micrometres before adsorption and 4.61 micrometres and 0.796 micrometres after adsorption, respectively.

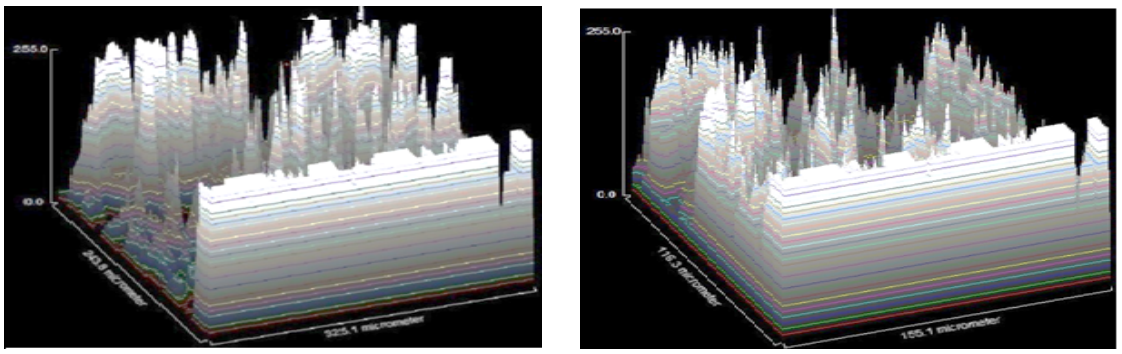

Zr-AAABC Before adsorption

Zr-AAABC after adsorption

Fig. 3. Surface analysis by ImageJ software

Energy-dispersive X-ray Spectroscopy analysis

The elemental composition of Zr-AAABC adsorbent was investigated by EDX both before and during the adsorption of F^- ions. The material's surface composition variations throughout the adsorption process were crucially revealed by this research when combined with Scanning Electron Microscopy (SEM).

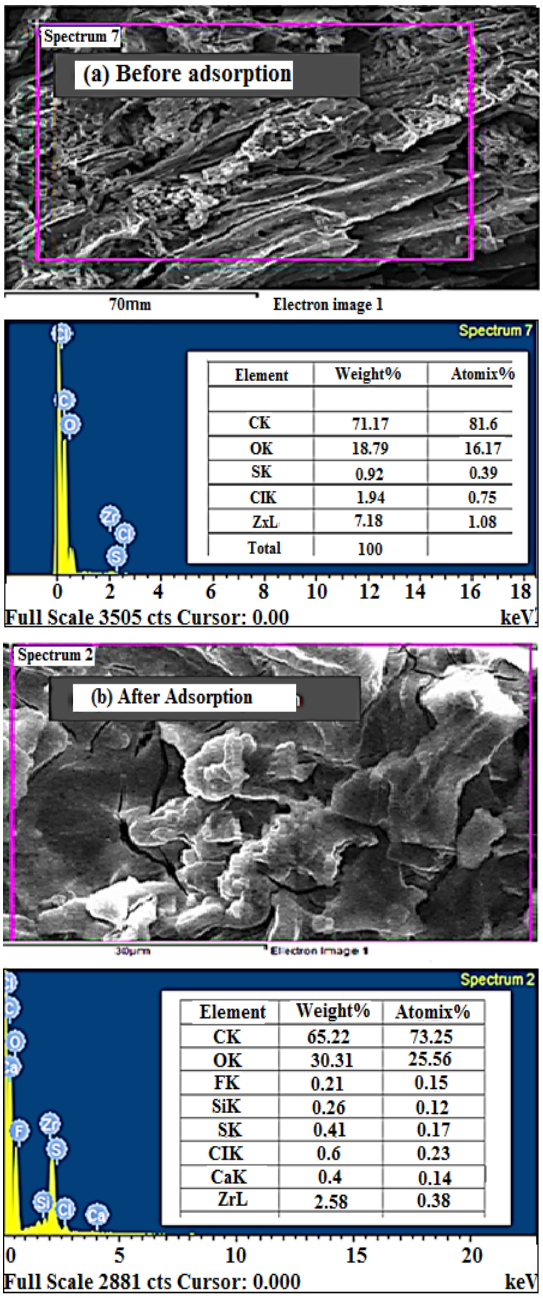

Fig. 4. Elemental analysis by EDX (Before and After Adsorption)

The EDX analysis of Zr-AAABC, as shown in the (Fig. 4), highlights the material's elemental composition before and after adsorption. Before adsorption, the peaks corresponding to C, O, Cl, S, and Zr confirm the successful embedding of zirconium on the surface of Zr-AAABC. This demonstrates that the Zr metal is well-integrated into the structure. After adsorption, a fluoride peak indicates the effective adsorption of fluoride ions onto the Zr-AAABC surface. Reduction in Zirconium, the decrease to 7.18 to 2.58 in weight% and 1.08 to 0.38% (atomix%) implies partial surface coverage by the adsorbed material, reducing the exposure of Zr. These results confirm the material's ability to interact with and adsorb fluoride, showcasing its functionality in adsorption applications.

Spectroscopic evidence for anchoring of Zr on AAABC and adsorption of fluoride on Zr-AAABC (FTIR analysis)

Spectroscopic analysis using FTIR was employed to investigate the fluoride adsorption mechanism on Zr-AAABC and the anchoring of Zr onto AAABC. The spectra (Fig. 5a) revealed that the peak at 3220.4 cm^{-1}, associated with –OH groups, shifted to 3239.1 cm^{-1} upon Zr addition (Fig. 5b), indicating an interaction between Zr and the –OH groups of AAABC. The significance of -OH groups in fluoride removal was further shown by the fact that the peak shift to 3324.8 cm^{-1} after adsorption of fluoride peak shift to 3324.8 cm^{-1} after fluoride adsorption (Fig. 5c). In addition, the peak at 1606.5 cm^{-1} is ascribed to carboxylate C=O stretching, and there is a shift from 1625.1 cm^{-1} to 1654 cm^{-1}, which shows functional group modifications after fluoride adsorption. The Zr-O and Zr-OH vibrations were reflected by the bands at 1264.2 cm^{-1} and 1375.4 cm^{-1}, respectively. A broad band at 1073.5 cm^{-1} suggested that the vibrations of the Zr-O, C-O, and Zr-OH bonds overlapped. These spectrum alterations demonstrate that Zr-AAABC's enhanced fluoride removal effectiveness is due to structural modifications and functional group interactions.

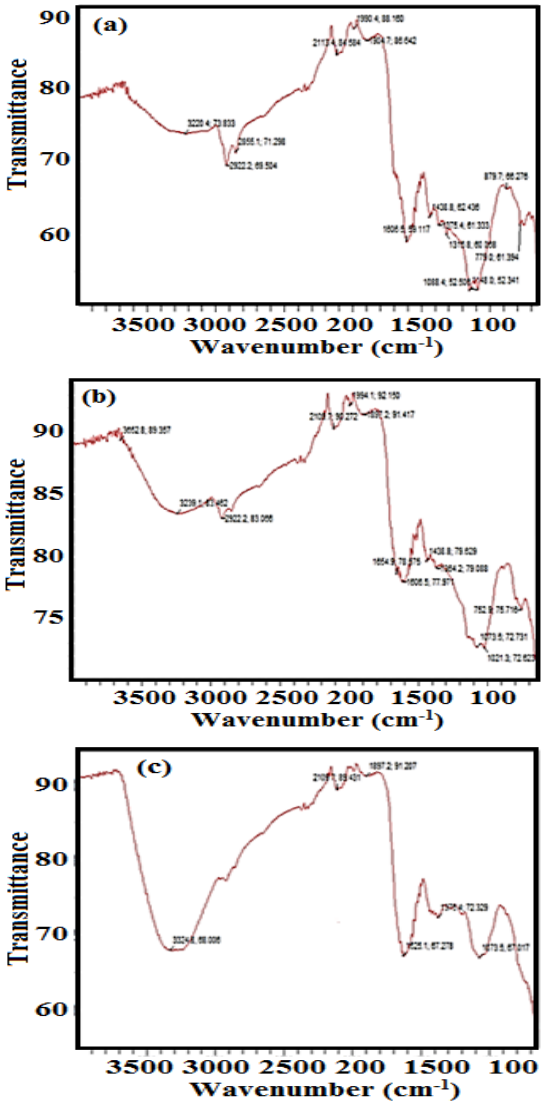

Fig. 5. FTIR spectra of (a) activated biochar of castor leaves (AB), (b) Zr-AAABC before fluoride adsorption and (c) Zr-AAABC after fluoride adsorption

Batch adsorption analysis

Fluoride Removal: Influence of Adsorbent Dose

Using a starting concentration of fluoride, 10 mg/L, a pH of 3, and Zr-AAABC amounts ranging from 0.1 to 1.5 g/L, adsorbent studies were carried out at 35°C for 2 hours. The fluoride elimination increased from 52% to 91.7%. We increased the number of doses from. 1 g to 1.5 g (Fig. 6a) due to more binding site availability at higher dosages. After reaching equilibrium at 1 g/L, saturation was achieved. So, we have used a dose of 1 g for our further studies.

Fluoride removal: Influence of duration of contact

The experiments were carried out at a temperature of 35°C using 1 g/L Zr-AAABC, 10 mg/L starting fluoride concentration, and pH level 3 to ascertain the minimum contact time required for optimal fluoride adsorption. As shown in the (Fig. 6b), the adsorption capacity levelled down after an initial surge in the first 120 min because as fluoride binds, the initial abundance of active sites is reduced. Two hours of contact time were used to ensure the attainment of equilibrium.

Fluoride removal: Influence of pH

Depending on the solution's pH, the adsorbent's functional groups are protonated differently. Experiments carried out at 35°C for 2 h with a concentration of 1 g/L Zr-AAABC and 10 mg/L fluoride solution showed that fluoride adsorption dropped significantly between pH 1 and 7 (Fig.6c). The creation of hydrofluoric acid in acidic circumstances enhanced fluoride removal, whereas the repulsion between fluoride and hydroxide ions in basic conditions inhibited it.

Fluoride removal: Influence of temperature

Figure 6d shows how the fluoride removal ability of Zr-AAABC changes with temperature. For two hours, starting with an initial concentration of 10 mg/L, pH 3, and 1 g/L adsorbent, the fluoride concentration was lowered by 89% by raising the temperature from 20°C to 60°C. However, increasing the temperature to 90°C decreased fluoride removal to 62%, likely due to increased fluoride ion solubility or enhanced escape from the Zr-AAABC surface.

Fluoride removal: Influence of initial concentration of fluoride

The study explored how fluoride's initial concentration (10-100 mg/L) affects Zr-AAABC's adsorption capacity. With 1 g/L adsorbent, pH 3, and 35°C for 2 h, maximum fluoride removal was observed at 10 mg/L. Higher concentrations reduced available active sites, decreasing fluoride removal, as shown in (Figure 6e).

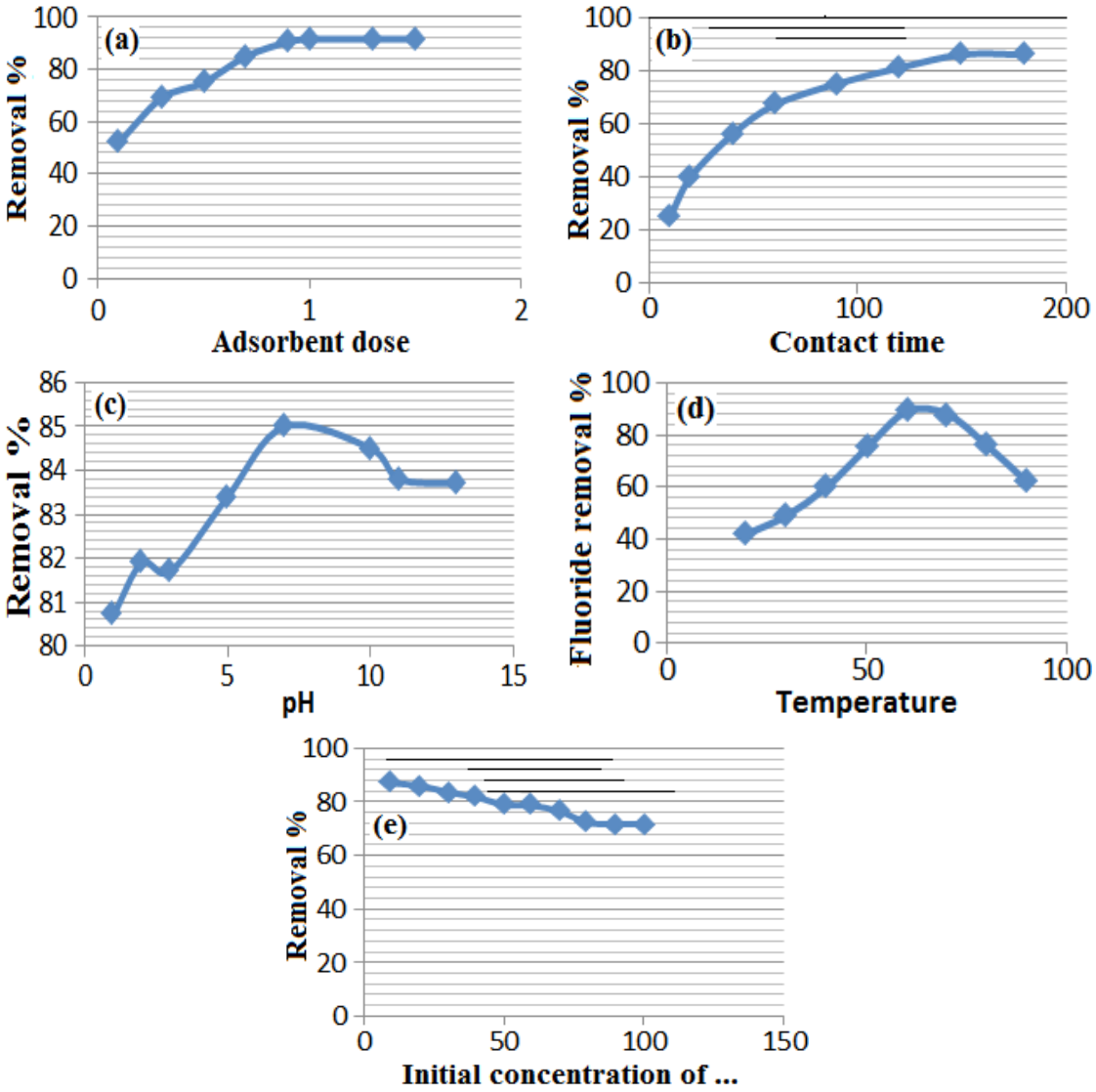

Fig. 6. Impact of (a) quantity of adsorbent, (b) contact duration, (c) pH, (d) temperature and (e) Initial F concentration on removal percentage of fluoride by Zr-AAABC

Adsorption equilibrium study

A study of adsorption equilibrium is crucial because it informs us how much adsorption will occur. The isotherm was used to identify the equilibrium parameters and adsorption characteristics[18]. It also shows how the adsorbent and adsorbate molecules interact. The fluoride adsorption mechanism onto Zr-AAABC is considered using Freundlich, Langmuir, and Temkin adsorption isotherms. The calculated adsorption isotherm values and the linearised type of these models are shown in Table 1.

Langmuir isotherm

It describes adsorption at homogeneous regions of the surface of the adsorbent[19]. The equation is expressed as:

$$1/q_e = 1/bq_{max}C_e + 1/q_{max}.$$

This equation states that the Langmuir constant (K_L) is equal to q_{max}, where C_e is adsorbate concentration at equilibrium in the liquid phase, q_e is the quantity of adsorbed adsorbate at equilibrium, and q_{max} is the sorption capacity of the monolayer at saturation point[20]. The equilibrium parameter, R_L, is obtained as follows:

$$R_L = 1/1 + K_L C_0$$

The Langmuir isotherm model was used to assess fluoride adsorption onto Zr-AAABC. The model's parameters are shown in Table 1, exhibiting a high correlation coefficient ($R^2 = 0.998$), suggesting a remarkable match to the Langmuir equation. The monolayer saturation capacity (q_m) was determined to be 9.183 mg/g. Given that it falls between 0 and 1, the dimensionless separation factor (R_L) value of 0.014527 suggests good adsorption circumstances. This indicates that the Langmuir model well describes the adsorption of fluoride on Zr-AAABC, which means that the adsorbent surface is effectively covered by a monolayer (Figure 7a).

Freundlich isotherm

In general, physicochemical adsorption on heterogeneous surface energy systems can be explained by the Freundlich isotherm[21]. The linear form is expressed as follows:

$$\log q_e = (1/n) \log C_e + \log K_f$$

K_f and n are Freundlich constant. A measure of surface heterogeneity, 1/n has a numerical value between 0 and 1. Surface heterogeneity is indicated by a value of 1/n closer to zero. A chemisorption process is marked by several 1/n less than 1, while cooperative adsorption is indicated by a 1/n more than 122 value. The plot's excellent linearity ($R^2 = 0.988$) suggests that this isotherm can be used effectively for fluoride sorption on Zr-AAABC surfaces (Fig. 7 b). The value of 1/n, or less than 1, (0.652) also suggested that Zr-AAABC and fluoride ions formed a substantially stronger link and had a better adsorption mechanism.

Temkin isotherm

The Temkin isotherm is typically employed for systems with heterogeneous surface energy. It facilitates the assessment of the adsorbed solution's and adsorbent's adsorption potential[23]. The free energy of sorption is assumed to be a function of surface coverage for the Temkin isotherm.

The Temkin isotherm's lineralized form is:

$$q_e = B \ln A_T + B \ln C_e$$

The adsorption enthalpy is related to B and calculated as RT/bT. The Temkin coefficient (mg/L) is abbreviated as A_T.

With K_T values of 0.8621 L/mg and BT values of 2.012 J/mol, together with an R^2 value of 0.958, the model seems suitable for fluoride adsorption on Zr-AAABC (Figure 7c).

Table 1: Isotherms of Zr-AAABC for F^- adsorption

Initial fluoride-concentration	Langmuir	Freundlich	Temkin
10 mg/L	q_m(mg/g) 9.18 K_L 6.78 R_L 0.014 $R^2$0.998	K_f 0.833 1/n 0.652 R^2 0.988	B_T(J/mol) 2.012 K_T(L/mg) 0.862 R^2 0.958

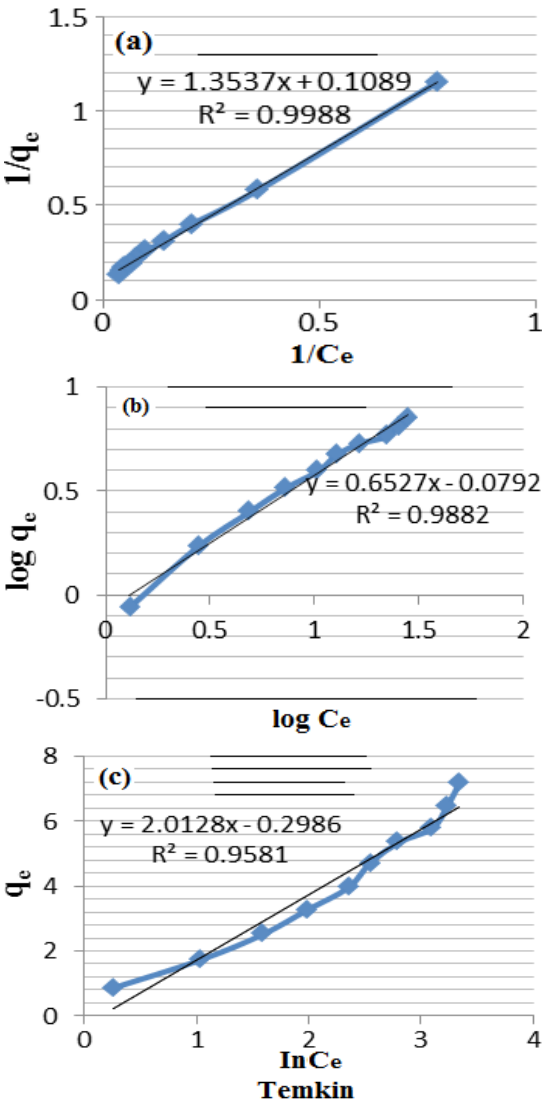

Fig. 7. Adsorption isotherm study

Adsorption kinetics

The kinetics of any adsorption process are contingent upon various factors, such as the

concentration of the adsorbate, the interactions between adsorbate and adsorbent, and the structural characteristics of the adsorbent[24]. These variables collectively influence how efficiently and rapidly adsorption occurs in a given system.

Pseudo-first order

The linear form of the pseudo-first-order ordermodel2025 is model is expressed as;

$$\log (q_e - q_t) = \log q_e - K_1 t/2.303$$

Here, K_1 is hypothetical first-order kinetic model rate constant (1/min), q_e is fluoride adsorption amount onto Zr-AAABC at equilibrium (mg/g), and qt is fluoride adsorption quantity onto Zr-AAABC at time t. Table 2 summarisesthe findings of the current study. According tothe graph of ln (q_e-q_t) vs t (Fig. 8a), values of K_1 and q_e are -0.000138 and 0.91 mg/g, respectively. As predicted by theory, the graph was linear (R^2 = 0.969). The computed values of q_e, which are 0.91 mg/g and q_e exp, which are 0.87 mg/g, showed the least difference between the two sets of values, suggesting that the first-order kinetics can be applied to fluoride adsorption by Zr-AAABC.

Pseudo-second order

This model's kinetic process is expressed as follows:

$$dq_1/d_t = K_2(q_e - q_t)^2$$

Here, K^2 is rate constant g/ (min. mg)[26].

Table 2 shows the values of K^2 and q_e, which were obtained by plotting t/q_t vs. t (Fig. 8b). A linear relationship between t/q_t and t was shown in the plots (R^2 = 0.981) when the second-order rate model was used under these circumstances.

Very few discrepancies exist between the experimental findings of q_e (0.87 mg/g) and the q_e value (0.95 mg/g) found in the second-order plot. This suggests that the second-order mechanism controls the fluoride adsorption process.

Intra-particle diffusion model

This model evaluates whether pore diffusion isthe limiting phase during adsorption[27]. The rate constant (K_{diff}, g/(mg.min$^{1/2}$)) of this model was determined using the following equation:

$$q_t = K_{dif} \cdot t^{1/2} + C$$

The model is used to analyse fluoride sorption on Zr-AAABC, focusing on boundary layer thickness (C) and k_{dif} (slope of q_t vs $t^{0.5}$ plot in g/(mg•min$^{0.5}$)). The Weber-Morris plot (Fig. 8c) demonstrated good linearity (R^2 = 0.955), with a zero intercept (0.076), indicating minimal boundary layer effects. This suggests that intra-particle diffusion likely governs the rate of fluoride accumulation on Zr-AAABC, validating the model's utility.

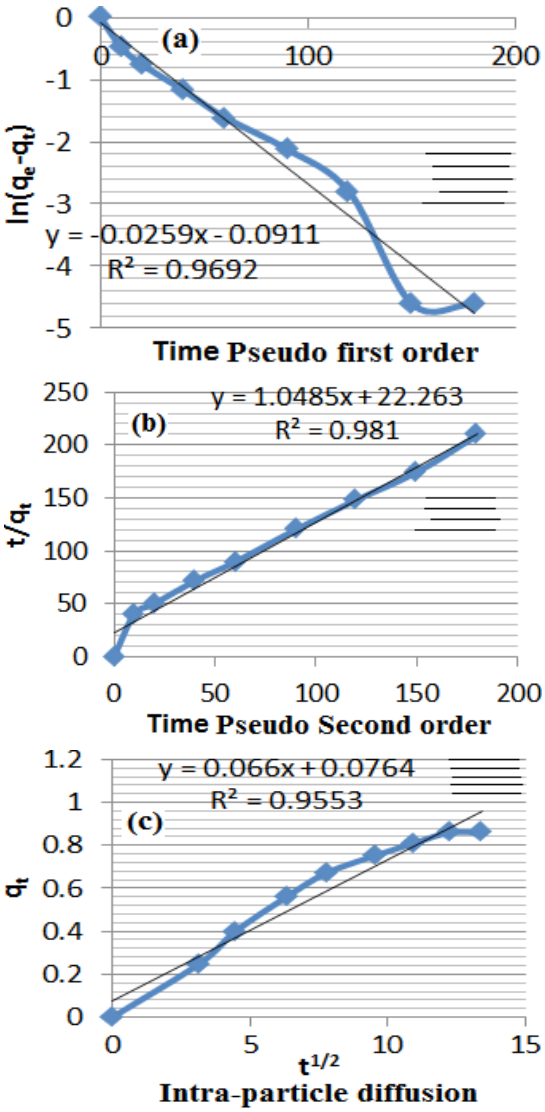

Fig. 8. Adsorption kinetic study of Zr-AAABC

Table 2: Reaction rates for Zr-AAABC adsorption on F-surface

Initial concentration	Pseudo first order	Pseudo second order	Intraparticle diffusion
10	q_e, exp(mg/g) o.87 q_e, cal (mg/g) 0.91 K_1 -.0001 R^2 0.969	q_e, cal (mg/g) 0.954 K_2 0.04 R^2 0.981	K_{diff} (g/(mg.min$^{1/2}$) 0.066 I. 076 R^2 0.955

CONCLUSION

The study effectively demonstrates the high efficiency of the Zr-AAABC adsorbent in removing excess fluoride from water. Under optimal conditions-pH 7, an adsorbent dose of 1 g/L, a contact time of 2 h, a temperature of 60°C, and an initial fluoride concentration of 10 mg/L-a fluoride removal efficiency of 92% was achieved using this simple yet promising approach. Modifying activated biochar with agar-agar and a zirconium-based bioadsorbent enhanced the efficiency from 82% to 92%. The experimental data align well with the pseudo-second-order kinetic model and the Langmuir adsorption isotherm, indicating that these models effectively describe the adsorption and reaction kinetics. These findings contribute significantly to fluoride removal technology, offering a practical and reliable solution for mitigating fluoride contamination in water resources.

ACKNOWLEDGEMENT

We are very grateful to PHED Jodhpur and Defence Laboratory Jodhpur for providing the facilities required for this investigation.

Conflict of interest

The authors declare no conflict of interest in the present research work.

REFERENCES

1. Ali S.; Shekhar S.; Chandrasekhar T.; Yadav A. K.; Arora N.; Kashyap C. A.; Chandrasekharam. D., Influence of the water-sediment interaction on the major ions chemistry and fluoride pollution in groundwater of the Older Alluvial Plains of Delhi, India., *J. Earth Sys. Sci.*, **2021**,*130*(2), 1-16.https://doi.org/10.1007/s12040-021-01585-3
2. Jain A.; Singh S., Prevalence of Fluoride in Ground Water in Rajasthan State: Extent, Contamination Levels and Mitigation,*Open J. Water Poll. Treat.*, **2014**, *2014*(2), 50–57,https://doi.org/10.15764/wpt.2014.02006
3. Adimalla N.; Qian H., Spatial distribution and health risk assessment of fluoride contamination in groundwater of Telangana: A state-of-the-art. *Geochemistry*, **2020**, *80*(4), 125548. https://doi.org/10.1016/j.chemer.2019.125548
4. Jain P. S.; Prasad S. B. B.; Raghu A. V., A short review: Removing fluoride ions from groundwaterusing various techniques., *Int. J. Res.-Granthaalayah.*, **2017**, *5*(4RAST), 98–104. https://doi.org/10.29121/granthaalayah.v5.i4rast.2017.3310
5. Habuda-Stani M.; Ravani M.; Flanagan A., A Review on Adsorption of Fluoride from Aqueous Solution.*, Materials.*, **2014**, *7*(9), 6317–6366. https://doi.org/10.3390/ma7096317
6. Ahmadijokani F.; Molavi H.; Rezakazemi M.; Aminabhavi T. M.; Arjmand M., Simultaneous detection and removal of fluoride from water using smart metal-organic framework-based adsorbents., *Coord. Chem. Rev.*, **2021**, *445*, 214037. https://doi.org/10.1016/j.ccr.2021.214037
7. Liu Z.; Zheng S.; Zhang D., Al-Impregnated Granular Activated Carbon for Removal of Fluoride from Aqueous Solution: Batch and Fixed-Bed Column Study., *Water.*, **2022**, *14*(21), 3554. https://doi.org/10.3390/w14213554
8. Liao X.; Shi B., Adsorption of Fluoride on Zirconium (IV)-Impregnated Collagen Fiber., *Environ. Sci. Tech.*, **2005**, *39*(12), 4628–4632. https://doi.org/10.1021/es0479944
9. Hu H.; Yang L.; Lin Z.; Zhao Y.; Jiang X.; Hou L., A low-cost and environment-friendly chitosan/aluminiumhydroxide bead adsorbent for fluoride removal from aqueous solutions. Iran., *Pol.J.*, **2018**, *27*(4), 253–261. https://doi.org/10.1007/s13726-018-0605-x

10. Pirsaheb M.; Mohammadi H.; Sharafi K.; Asadi A., Fluoride and nitrate adsorption from water by Fe(III)-doped scoria: optimising using response surface modelling, kinetic and equilibrium study., *Water Supp.*, **2017**, *18*(3), 1117–1132. https://doi.org/10.2166/ws.2017.185
11. Saidi S.; Farouk B.; Idris Y.; Farida A. B., Agar-agar impregnated on porous activated carbon as a new Pb(II) removal adsorbent., *Water Sci. Technol.*, **2019**, *79*(7), 1316–1326. https://doi.org/10.2166/wst.2019.128
12. Tripathy, S. S.; Bersillon, J. L., & Gopal, K., Removal of fluoride from drinking water by adsorption onto alum-impregnated activated alumina., *Bioresource Technology.*, **2006**, *97*(5), 924-930.
13. Zhang, Y.; Jia, Y., & Wang, H., Removal of fluoride from water using zirconium-based adsorbents: *A review. Separation and Purification Technology*, **2011**, *83*(1), 66-73.
14. Ma, W., Ya, F., Zhang, C., & Liu, Y., Enhanced fluoride adsorption on zirconium-modified biochar derived from agricultural waste., *Chemical Engineering J.,* **2019**, *362*, 295-305.
15. Ghosh, D.; Medhi, C., & Purkait, M. K., Treatment of fluoride-containing drinking water by adsorption onto Zr(IV)-impregnated activated carbon., *Separation Science and Technology.*, **2008**, *43*(14), 3673-3691.
16. Singh S.; German M.; Chaudhari S.; Sengupta A.K. Fluoride Removal from Groundwater using Zirconium Impregnated Anion Exchange Resin., *J. Environ. Manag.*, **2020**, *263*, 110415. DOI: 10.1016/j.jenvman.2020.110415.
17. Arezo S.; Hashemi S.; Hossein A.; Dobaradaran S.; Foroutan R.; Amir H. M.; Bahman R., Physicochemical characteristics and mechanism of fluoride removal using powdered zeolite-zirconium in modes of pulsed & continuous sonication and stirring., *Adv. Pow. Tech.*, **2020**, *31*(8), 3521–3532. https://doi.org/10.1016/j.apt.2020.06.039
18. Raul P. K.; Devi R. R.; Umlong I. M.; Banerjee S.; Singh L.; Purkait, M., Removal of Fluoride from Water Using Iron Oxide-Hydroxide Nanoparticles., *J. Nanosci. Nanotech.*, **2012**, *12*(5), 3922–3930. https://doi.org/10.1166/jnn.2012.5870
19. Suneetha M.; Sundar B. S.; Ravindhranath K., Removal of fluoride from polluted waters using active carbon derived from barks of Vitex negundo plant., *J. Anal. Sci. Technol.*, **2015**, *6*(1).https://doi.org/10.1186/s40543-014-0042-1
20. Thouraya T.; Abdelkader H.; Alexandru E., Fluoride Adsorption from Aqueous Solution by Modified Zeolite-Kinetic and Isotherm Studies., *Molecules.*, **2023**, *28*(10), 4076–4076. https://doi.org/10.3390/molecules 28104076
21. Krishnamurthy P. A.; Nakajima H.; Rashid S. A., Adsorptive, kinetics and regeneration studies of fluoride removal from water using zirconium-based metal-organic frameworks., *RSC Adv.*, **2020**, *10*(32), 18740–18752. https://doi.org/10.1039/d0ra01268h
22. Daifullah A.; Yakout S.; Elreefy S., Adsorption of fluoride in aqueous solutions using KMnO4-modified activated carbon derived from steam pyrolysis of rice straw., *J. Haz. Mat.*, **2007**, *147*(1-2), 633–643. https://doi.org/10.1016/j.jhazmat.2007.01.062
23. Singh K.; Lataye D. H.; Wasewar K. L., Removal of Fluoride from Aqueous Solution by Using Low-Cost Sugarcane Bagasse: Kinetic Study and Equilibrium Isotherm Analyses., *J. Haz. Tox. Rad. Was.*, **2016**, *20*(3), 04015024. https://doi.org/10.1061/(ASCE)hz.2153-5515.0000309
24. Zarrabi M.; Samadi M. T.; Sepehr M. N.; Ramhormozi S. M.; Azizian S.; Amrane A., Removal of fluoride ions by ion exchange resin: kinetic and equilibrium studies, Env., *Engin. Manag. J.*, **2014**, *13*(1), 205–214. https://doi.org/10.30638/eemj.2014.025
25. Ramanaiah S. V.; Venkata M. S.; Sarma P. N., Adsorptive removal of fluoride from aqueous phase using waste fungus (Pleurotus ostreatus 1804) biosorbent: Kinetics evaluation., *Ecol. Engin.*, **2007**, *31*(1), 47–56. https://doi.org/10.1016/j.ecoleng.2007.05.006
26. Yousefi M.; Arami S. M.; Takallo H.; Hosseini M.; Radford M.; Soleimani H.; Mohammadi A. A., Modification of pumice with HCl and NaOH enhancing its fluoride adsorption capacity: Kinetic and isotherm studies., *Human Ecol. Risk Assess: An Int. J.*, **2018**, *25*(6), 1508–1520. https://doi.org/10.1080/10807039.2018.1469968
27. Mohammad H. D.; Faraji M.; Mohammadi A.; Kamani H., Optimization of fluoride adsorption onto natural and modified pumice using response surface methodology: Isotherm, kinetic and thermodynamic studies., *Kor. J. Chem. Engin.*, **2016**, *34*(2), 454–462. https://doi.org/10.1007/s11814-016-0274-4